

# Nonlinear Analysis of Renal Autoregulation in Rats Using Principal Dynamic Modes

VASILIS Z. MARMARELIS,<sup>1</sup> KI H. CHON,<sup>2</sup> NIELS H. HOLSTEIN-RATHLOU,<sup>3</sup> and DONALD J. MARSH<sup>2</sup>

<sup>1</sup>Department of Biomedical Engineering, University of Southern California, Los Angeles, CA,

<sup>2</sup>Department of Molecular Pharmacology, Physiology and Biotechnology, Brown University, RI, and

<sup>3</sup>Department of Medical Physiology, University of Copenhagen, Copenhagen, Denmark

(Received 31 December 1997; accepted 11 August 1998)

**Abstract**—This article presents results of the use of a novel methodology employing principal dynamic modes (PDM) for modeling the nonlinear dynamics of renal autoregulation in rats. The analyzed experimental data are broadband (0–0.5 Hz) blood pressure-flow data generated by pseudorandom forcing and collected in normotensive and hypertensive rats for two levels of pressure forcing (as measured by the standard deviation of the pressure fluctuation). The PDMs are computed from first-order and second-order kernel estimates obtained from the data via the Laguerre expansion technique. The results demonstrate that two PDMs suffice for obtaining a satisfactory nonlinear dynamic model of renal autoregulation under these conditions, for both normotensive and hypertensive rats. Furthermore, the two PDMs appear to correspond to the two main autoregulatory mechanisms: the first to the myogenic and the second to the tubuloglomerular feedback (TGF) mechanism. This allows the study of the separate contributions of the two mechanisms to the autoregulatory response dynamics, as well as the effects of the level of pressure forcing and hypertension on the two distinct autoregulatory mechanisms. It is shown that the myogenic mechanism has a larger contribution and is affected only slightly, while the TGF mechanism is affected considerably by increasing pressure forcing or hypertension (the emergence of a second resonant peak and the decreased relative contribution to the response flow signal). © 1999 Biomedical Engineering Society. [S0090-6964(99)00201-5]

**Keywords**—Nonlinear modeling, Volterra kernels, Laguerre expansion.

## INTRODUCTION

Two primary mechanisms are thought responsible for renal autoregulation (i.e., the process by which vascular hemodynamic impedance is adjusted to minimize fluctuations in blood flow caused by fluctuations in blood pressure): the myogenic mechanism and the tubuloglomerular feedback (TGF).<sup>3–7</sup> The myogenic mechanism is vascular in nature and causes changes in the blood vessel diameter and mechanical characteristics (e.g., stiffness)

in response to changes in local vascular pressure. The TGF mechanism is governed by flow-rate dependent concentration changes in tubular fluid (sensed at the distal tubular site, the macula densa) and alters the impedance characteristics of the preglomerular vessels through still unknown signals that affect vascular smooth muscle. The frequency response characteristics of the two mechanisms have been studied in rats,<sup>3–5,7,18</sup> and the consensus is that the myogenic mechanism is faster and is associated with a resonance (decreased impedance) over the frequency range from 0.08 to 0.16 Hz. The TGF mechanism is active for frequencies below 0.08 Hz and is associated with a strong resonance between 0.02 and 0.05 Hz, where it exhibits an intrinsic, self-sustained oscillation.<sup>6,7</sup> The combined action of the two mechanisms attenuates the effect of blood pressure fluctuations on blood flow at frequencies less than 0.08 Hz, where most of the naturally occurring power is found in the blood pressure spectrum.<sup>17</sup>

Recent studies in rats have used externally imposed broadband arterial pressure fluctuations to separate the dynamical properties of the two renal autoregulatory mechanisms.<sup>3,4,16</sup> The advantages of broadband forcing as an excitation in linear and nonlinear system identification have been well documented, and the associated modeling techniques have gained in popularity over the last 25 years.<sup>8–11,13,14</sup> Suppression of noise and reduction of experimentation time are among these advantages. Another major advantage is the ability of this approach to discern quantitatively the linear and nonlinear dynamic characteristics of the system under study by means of Volterra kernels.<sup>8,19</sup>

In previous papers, we presented nonlinear Volterra models of renal autoregulation in rats and explored the physiological interpretation of the obtained Volterra kernels.<sup>16</sup> A third-order Volterra model was shown to be adequate in representing the dynamic relationship between renal blood flow and arterial pressure in a broadband context up to 1 Hz.<sup>4,16</sup> The effects of increasing power in broadband pressure forcing were examined and

Address correspondence to Prof. Vasilis Marmarelis, Department of Biomedical Engineering, University of Southern California, University Park—OHE 500, Los Angeles, CA 90089-1451. Electronic mail: vzm@bmsrs.usc.edu

shown to cause increased damping of the system dynamics in a manner consistent with the presence of nonlinear compressive (sigmoid) feedback.<sup>12</sup> The nonlinear interaction between the two primary autoregulatory mechanisms (the myogenic and TGF) were examined by means of the experimentally obtained second-order and third-order Volterra kernels.<sup>4</sup> Distinct differences in such nonlinear interactions were observed between normotensive and hypertensive rats. Specifically, such interaction was most evident for low-level forcing in normotensive rats. The nonlinear dynamic characteristics of each individual mechanism changed for different levels of pressure forcing and between normotensive and hypertensive rats.<sup>4,16</sup>

Although these studies represent significant progress in understanding the nonlinear dynamic characteristics of renal autoregulation under broadband conditions, the subtle changes in the characteristics of the individual mechanisms (myogenic and TGF) with varying pressure forcing level or between normotensive and hypertensive rats require further analysis. This is pursued in this article by means of the recently introduced “principal dynamic mode” (PDM) analysis for nonlinear physiological systems.<sup>15</sup> It is shown that two PDMs obtained from the experimentally measured kernels appear to correspond to the two autoregulatory mechanisms in terms of the respective frequency band of operation—a fact that allows a more precise analysis of the aforementioned changes in the characteristics of the two mechanisms.

In the following section the experimental preparation and data collection procedures are described briefly. The Methodology section contains an outline of the PDM approach. In the Results section the results obtained are presented, and the main conclusions are summarized in the final section.

## DATA COLLECTION

Experiments were performed on three male spontaneously hypertensive rats (SHRs) and on three age-matched male normotensive Sprague-Dawley rats (SDRs) weighing 250–350 g. The animals had free access to food and tap water prior to the experiments. The experimental procedure is described in detail elsewhere.<sup>3,4,16</sup> In brief, the rats were anesthetized with halothane administered in an oxygen-nitrogen mixture and were artificially ventilated after the administration of a muscle relaxant (gallamine triethiodide). The abdomen was opened through a midline incision extended to the left flank, and the distal aorta was cannulated at the bifurcation with a Teflon tube filled with blood freshly obtained from a littermate. The catheter was connected to a steel bellows pump. The left kidney was denervated, and an electromagnetic flow probe was placed around the left renal artery for measurements of flow. The arterial pressure was measured in the superior mesenteric artery.

Measurements of blood flow and blood pressure were made while broadband fluctuations were induced in the arterial blood pressure by a bellows pump. The linear motor that moved the bellows was driven by a power amplifier controlled by a personal computer through a digital-to-analog (D/A) converter. The input to the D/A converter was a constant-switching-pace symmetric random signal (CSRS), which exhibits the spectral properties of band-limited white noise.<sup>9</sup> Two different levels of arterial pressure forcing (measured by the standard deviation of the resulting pressure fluctuations) were used. The power levels varied somewhat from experiment to experiment, but two clusters of arterial pressure levels were roughly formed for both the SDRs and the SHRs.<sup>4</sup>

The renal blood flow and arterial pressure signals were sampled over 256 s with a sampling rate of 2 samples/s (Nyquist frequency of 1 Hz), after digital low-pass filtering to avoid aliasing. For the purposes of this study, we chose to further limit the data bandwidth to 0.5 Hz (down sampling by a factor of 2 after low-pass filtering at 0.5 Hz) in order to focus more on the frequency band of interest to autoregulation. Recall that above 0.4 Hz the system exhibits “all-pass” characteristics with no autoregulation dynamics in evidence. Each time series was subjected to second-degree polynomial trend removal. In addition, each data record containing 256 data points was demeaned (by subtracting out the mean value) and normalized by dividing with the standard deviation value of each data record. Thus, regardless of differences in the arterial pressure forcings, all analyzed data sets had zero mean and unit variance since our interest is focused on the dynamic characteristics of autoregulation, irrespective of relative scaling factors from experiment to experiment.

## METHODOLOGY

The general methodology of nonlinear modeling of dynamic systems using functional expansions and kernels has its origin in Wiener’s pivotal monograph that suggested the use of Gaussian white noise (GWN) as the effective test input for nonlinear system identification based on a hierarchy of nonlinear functionals (the Wiener series).<sup>21</sup> Volterra’s pivotal contribution was in suggesting, much earlier, the use of functional expansions (the Volterra series) to represent unknown analytic functionals implicated in studies of nonlinear mechanics and population dynamics.<sup>19</sup> As the Volterra-Wiener theories were gradually adapted to actual applications, discrete-time representations of the functionals and finite-bandwidth approximations of the input GWN signals became practically necessary. The fundamental importance of this problem and the generality of the Volterra-Wiener approach gave rise to a host of innova-

tive variants and implementations of this approach in applications to physiological system modeling (for a partial review, see Refs. 8–16).

In discrete time, the general input-output relation of a stable (finite-memory) nonlinear time-invariant dynamic system is given by the discrete-time Volterra series:

$$y(n) = k_0 + \sum_m k_1(m)x(n-m) + \sum_{m_1} \sum_{m_2} k_2(m_1, m_2)x(n-m_1)x(n-m_2) + \dots, \quad (1)$$

where  $x(n)$  is the input and  $y(n)$  is the output of the system. The Volterra kernels  $(k_0, k_1, k_2, \dots)$  describe the dynamics of the system from a hierarchy of system nonlinearities.

Expansion of the Volterra kernels on a complete basis  $\{b_j(m)\}$  transforms Eq. (1) into the multinomial expressions

$$y(n) = c_0 + \sum_j c_1(j)v_j(n) + \sum_{j_1} \sum_{j_2} c_2(j_1, j_2)v_{j_1}(n)v_{j_2}(n) + \dots = f(v_1, v_2, \dots, v_j, \dots), \quad (2)$$

where

$$v_j(n) = \sum_m b_j(m)x(n-m), \quad (3)$$

and  $c_1(j)$ ,  $c_2(j_1, j_2)$ , etc., represent the expansion coefficients of the respective kernels. The use of the kernel expansion basis implies that a general model of the Volterra class of systems can take the block-structured form of Fig. 1, wherein the basis functions  $\{b_j(m)\}$  constitute the impulse responses of a filter bank  $\{L_j\}$  whose outputs are feeding into the multi-input static nonlinearity  $f(v_1, \dots, v_j, \dots)$ . Wiener suggested the use of Laguerre functions as an appropriate orthonormal basis  $\{b_j(m)\}$ , owing to their built-in exponential term that makes them suitable for physical systems with asymptotically exponential relaxation dynamics. This suggestion was adopted in pioneering applications<sup>1,20</sup> and has been adapted to discrete time for improved kernel estimation from sampled data.<sup>13</sup> For a selected basis (e.g., Laguerre functions), the modeling problem reduces to estimating the multivariate function  $f(\bullet)$ .

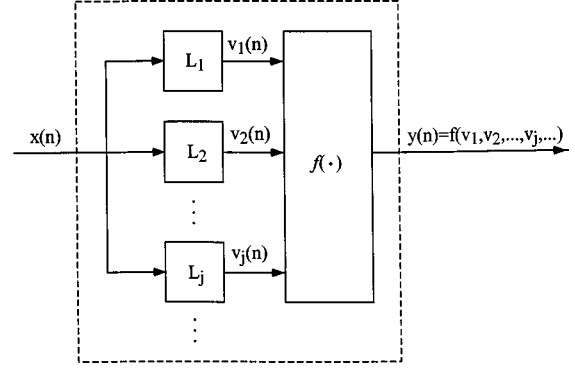


**FIGURE 1. Block-structured model for the general nonlinear Volterra system. The filter-bank outputs  $\{v_j\}$  feed into the multi-input static nonlinearity  $f(\bullet)$  that generates the system output.**

The proposed methodology of PDM analysis rests on the fact that, among all possible choices of expansion bases (orthogonal or nonorthogonal), there are some that require the minimum number of basis functions to achieve a given mean-square approximation of the system output. Such a minimum set of basis functions is termed PDMs of the nonlinear system and correspond to an associated multivariate nonlinear function  $f(\bullet)$  generating the system output. No claim of uniqueness can be made for these PDMs, in general. However the associated nonlinear function  $f(\bullet)$  is unique for a selected set of PDMs for a given system and vice versa.

The key practical issue is how to determine the minimum number of PDMs required in a given modeling application and how to estimate the corresponding static nonlinearities (of arbitrary order) from stimulus-response data. The methodology is detailed in Ref. 15.

The eigendecomposition method of PDM estimation was selected for this application because it yielded more consistent results (for different preparations) than the artificial neural network method. Although the methodology has been presented before, we provide an outline in the Appendix for the convenience of the reader.

## RESULTS

We begin with PDM analysis of six normotensive (SDR) input–output datasets, each having 256 datapoints sampled every 1 s, that were collected in two clusters of three under conditions of medium and high pressure forcing (as measured by the standard deviation of the applied pressure broadband perturbation). The kernel estimates from these data (although for the broader bandwidth of 1 Hz) using the Laguerre expansion technique have been reported before.<sup>16</sup> Using the PDM analysis methodology outlined in the Appendix (for  $M=50$ ) and employing seven Laguerre functions (with  $\alpha=0.5$ ), we obtain two PDMs that have fairly consistent

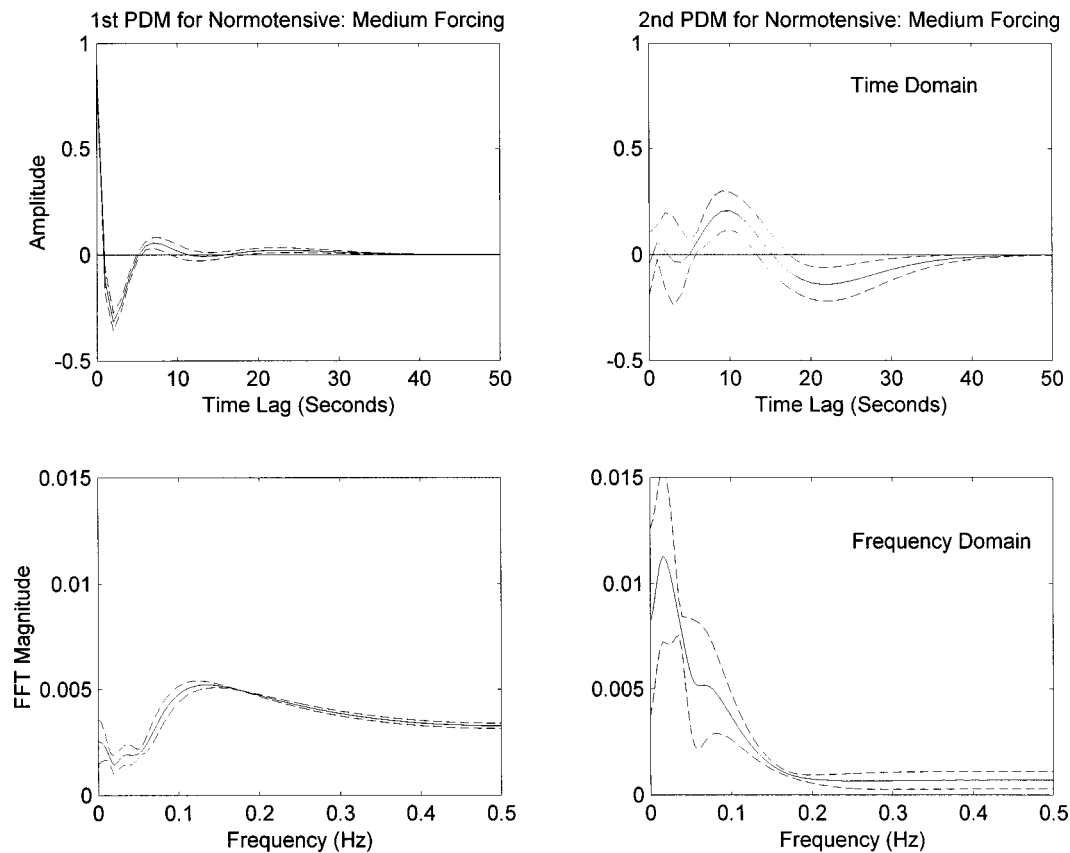


**FIGURE 2.** The two obtained PDMs of renal autoregulation (averaged over three data records) for the medium-forcing normotensive data in the time domain (top panels) and in the frequency domain (bottom panels). The first PDM (left panels) corresponds to the myogenic mechanism with a resonance peak around 0.12 Hz, and the second PDM (right panels) corresponds to the TGF mechanism with a resonance peak around 0.025 Hz. The standard error bounds in dashed lines correspond to  $\pm$  one standard deviation. The time-domain result is given by Eq. (A5).

wave forms for all experiments. Naturally, some limited variability is observed in the PDM wave forms across experiments at the same level of forcing, but the main dynamic characteristics (e.g., frequency band of characteristic resonant response) remain the same. Furthermore, these common dynamic characteristics across experiments for each of the two PDMs seem to correspond to the main frequency-response characteristics of the two autoregulatory mechanisms; viz., resonant peaks in the frequency bands: 0.08–0.16 Hz for the myogenic (first PDM) and 0.02–0.08 Hz for the TGF mechanism (second PDM). This is illustrated in Fig. 2, where the averages over three experiments of the two estimated PDMs for medium forcing are shown in the time and frequency domains. Additional PDMs corresponding to smaller eigenvalues exhibit mixed dynamic characteristics (i.e., resonant peaks at both frequency bands—myogenic and TGF). Occasionally, the second PDM exhibits this type of mixed dynamic characteristics and the third PDM then corresponds to the TGF mechanism. Additionally, linearly dependent PDMs may arise because of the first-element truncation described by Eq. (A5), which can lead to

different linear combinations for different values of the zero-order kernel (constant  $k_0$ ). We conjecture that the two PDMs correspond approximately to the two autoregulatory mechanisms—a conjecture that, if true, affords for the first time a detailed and separate analysis of the distinct dynamics associated with each of the two autoregulatory mechanisms.

We make use of this fact in order to examine the relative effect of the pressure forcing level on the two autoregulatory mechanisms by comparing the PDMs obtained for medium and high level of forcing in normotensive rats. The first PDM remains roughly the same for different levels of forcing, except for very low frequencies (below 0.02 Hz) where other extraneous factors are active, but are unrelated to renal autoregulation. The second PDM, however, changes significantly by exhibiting another strong resonant peak at the high end of the TGF frequency band (0.06–0.08 Hz). This may be the second harmonic of the fundamental frequency of the aforementioned intrinsic oscillation of the TGF (typically observed between 0.02 and 0.05 Hz), caused possibly by a saturation nonlinearity at high forcing levels. These

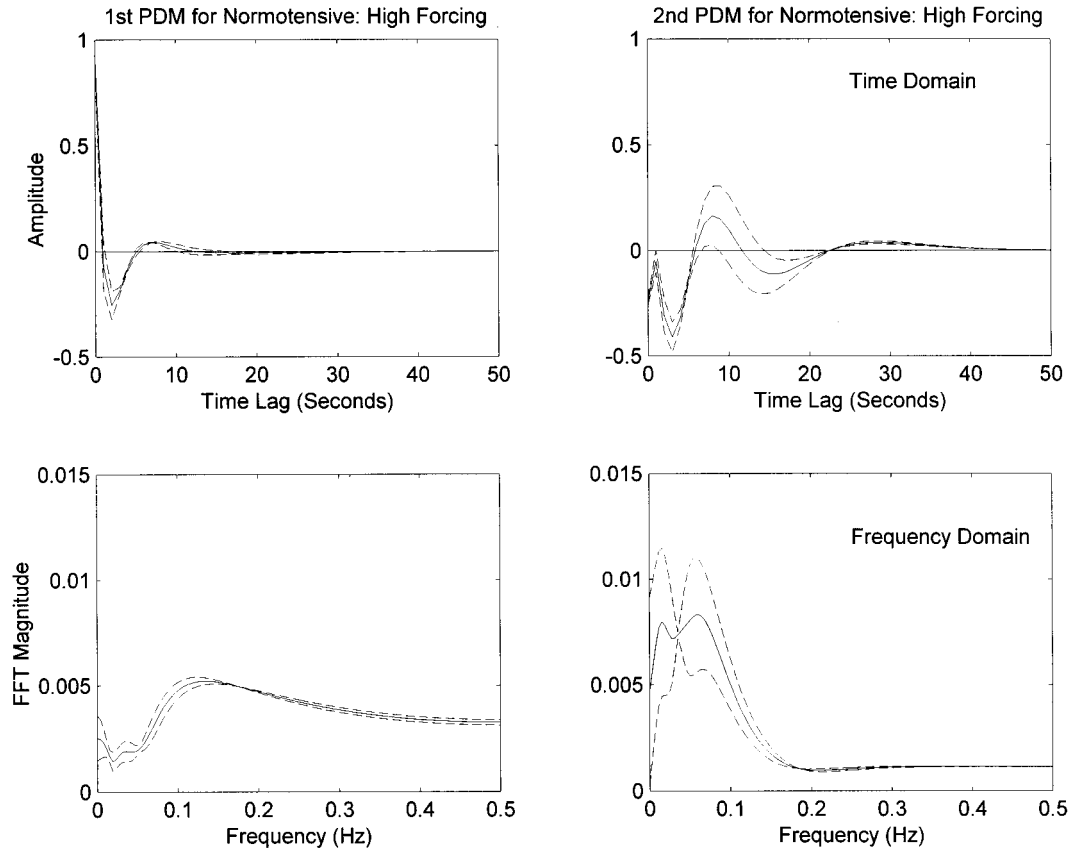


FIGURE 3. The two obtained PDMs (averaged over three data records) for the high-forcing normotensive data in the time domain (top panels) and in the frequency domain (bottom panels). The first PDM (left panels) corresponds to the myogenic mechanism and the second PDM (right panels) corresponds to the TGF mechanism of renal autoregulation. Compared to the medium-forcing case of Fig. 2, the first PDM has not been altered significantly but the second PDM exhibits marked changes (two resonant peaks at about 0.02 and 0.06 Hz). The standard error bounds in dashed lines correspond to  $\pm$  one standard deviation. The time-domain result is given by Eq. (A5).

facts are illustrated by comparing Fig. 2 with Fig. 3, where the average PDM estimates for medium and high levels of forcing in normotensive rats are presented.

It is important to note that the contribution to the system output of the first PDM (corresponding primarily to the myogenic mechanism) is about one order of magnitude larger than the contribution of the second PDM (corresponding primarily to the TGF mechanism) in normotensive rats, as indicated by the respective eigenvalues. The initial spike in the first PDM probably reflects the operation of elastic components in the vascular wall to the response. If this initial response is removed, the magnitude of the eigenvalue corresponding to the first PDM is still about five times that of the second. Furthermore, the estimated nonlinearities that are associated with each PDM show that the second PDM exhibits stronger nonlinear characteristics than the first PDM (relative to the respective linear terms). Weak interaction terms between the first PDM and the second PDM are also evident. These facts remain unaltered for different

levels of forcing in normotensive rats. For each experimental record, the two mode outputs ( $u_1, u_2$ ) can be computed and a polynomial function of ( $u_1, u_2$ ) can be fitted by least-squares regression to the system output. Orthogonal forward regression methods can be used to assess the statistical significance of these polynomial coefficients.<sup>2,22</sup> The normalized mean-square error of the third-order model prediction based on these two PDMs is about 12% for the medium-forcing data and below 5% for the high-forcing data (the latter corresponding to a case of higher signal-to-noise ratio in the data).

We repeat this PDM analysis for the two respective sets of hypertensive data. The average two PDMs for medium-level forcing are shown in Fig. 4 and appear similar to their normotensive counterparts for high-level forcing. However, the model prediction error is considerably higher in this case (approximately by a factor of 4 relative to the medium-forcing normotensive data), probably due to the chaotic spontaneous TGF oscillation observed in hypertensive rats.<sup>6</sup> The relative contributions of

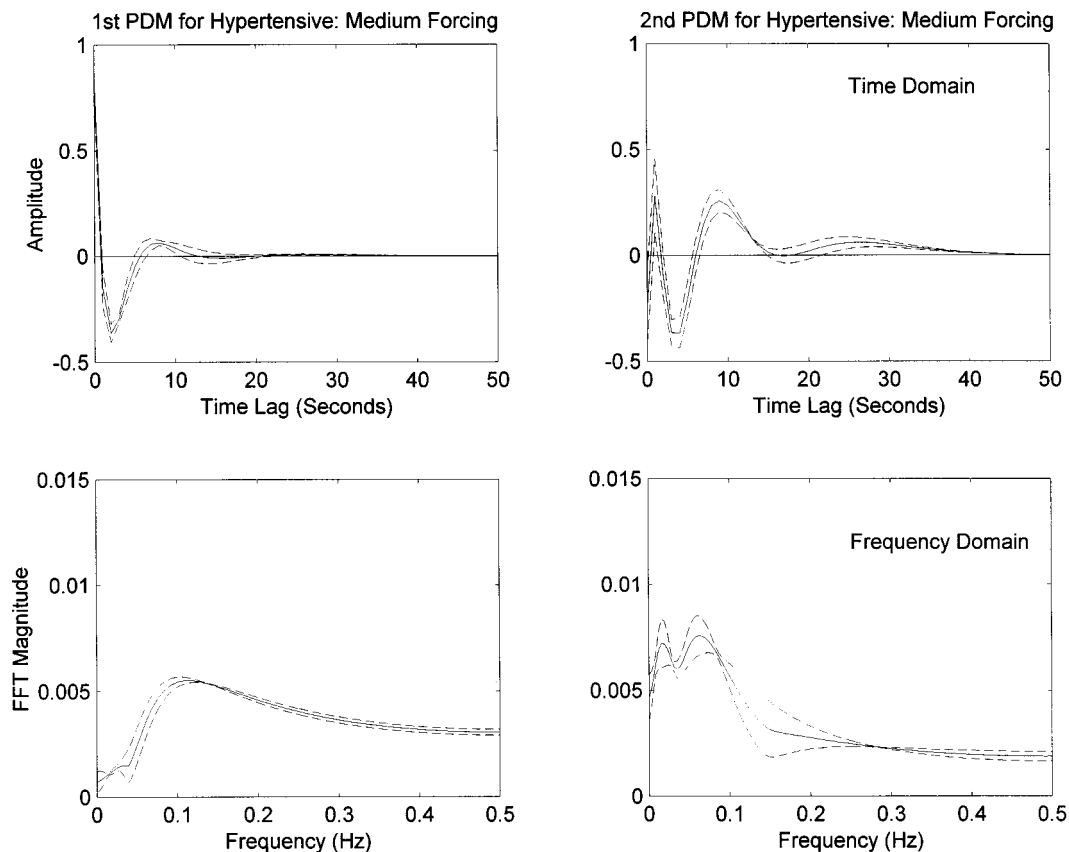


**FIGURE 4.** The two obtained PDMs (averaged over three data records) for the medium-forcing hypertensive data in the time domain (top panels) and in the frequency domain (bottom panels). The first PDM (left panels) corresponds to the myogenic mechanism and the second PDM (right panels) corresponds to the TGF mechanism of renal autoregulation. The first PDM is similar to the normotensive case (Figs. 2 and 3) and the second PDM resembles the high-forcing normotensive case (Fig. 3). The standard error bounds in dashed lines correspond to  $\pm$  one standard deviation. The time-domain result is given by Eq. (A5).

the two PDMs to the system output and the form of their respective nonlinearities for the medium-level hypertensive data are similar to the normotensive cases. For high-forcing conditions in hypertensive rats, however, the first PDM becomes dominant—a fact that suggests that the stimulus-coherent TGF response diminishes under these conditions—and the model prediction error is reduced by half. The average PDMs obtained for high-forcing conditions are shown in Fig. 5.

## CONCLUSIONS

The results demonstrate the efficacy of PDM analysis of renal autoregulation dynamics using broadband pressure-flow data. Two PDMs have been consistently identified in both normotensive and hypertensive rats for two levels of pressure forcing (as measured by the standard deviation of the applied pressure perturbation). These two PDMs correspond roughly to the two primary autoregulatory mechanisms (myogenic and TGF) as indicated by the respective frequency-response characteris-

tics. The contribution to the system output of the first PDM (corresponding to the myogenic mechanism) is several times larger than the contribution of the second PDM (corresponding to the TGF mechanism) in all cases, with the hypertensive high-forcing case exhibiting an even more dominant first PDM contribution to the system output.

Cubic nonlinearities were estimated for all cases (consistent with previous findings of third-order nonlinearities in this system) yielding models of good prediction accuracy, especially in the high-forcing cases owing to the higher signal-to-noise ratio. For medium and high pressure forcing, the normotensive models exhibit greater prediction accuracy than their hypertensive counterparts. Based on the estimated nonlinearities, the contribution of the second PDM is evidently more nonlinear than the first PDM contribution (relative to their respective linear contributions). Increasing the level of pressure forcing seems to affect primarily the second PDM (TGF mechanism) in both normotensive and hypertensive rats. In the high-forcing hypertensive case, the relative contribution

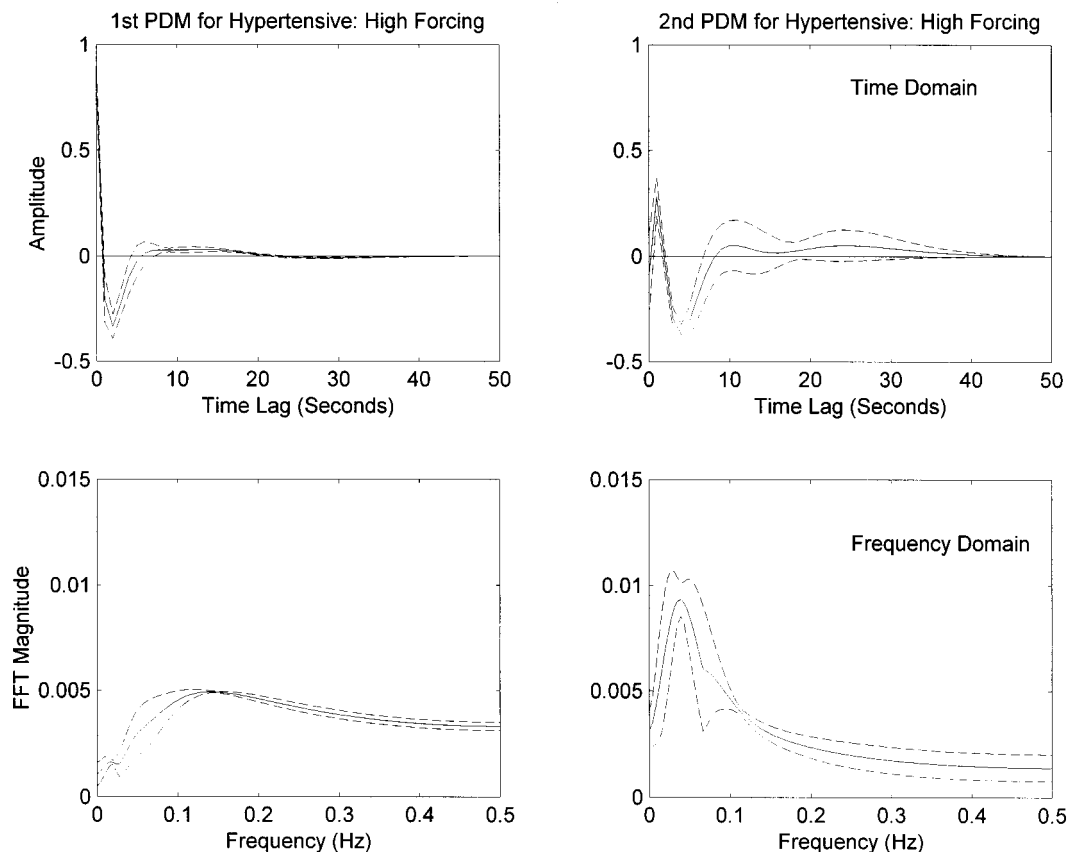


FIGURE 5. The two obtained PDMs (averaged over three data records) for the high-forcing normotensive data in the time domain (top panels) and in the frequency domain (bottom panels). The first PDM (left panels) corresponds to the myogenic mechanism and the second PDM (right panels) corresponds to the TGF mechanism of renal autoregulation. Only changes in the second PDM are evident relative to the medium-forcing hypertensive case (Fig. 4). The standard error bounds in dashed lines correspond to  $\pm$  one standard deviation. The time-domain result is given by Eq. (A5).

of the second PDM to the system output is reduced and its resonance shifts to the high end of the TGF band (0.06–0.07 Hz), while the first PDM contribution to the system output becomes dominant over the second PDM contribution. The two PDMs are similar in form in the cases of high-forcing normotensive and medium-forcing hypertensive data.

It is important to note that the reduced relative importance of the second PDM (corresponding to the TGF mechanism) in hypertensive rats does not imply a diminished role of the TGF mechanism overall. On the contrary, the role of TGF in hypertensive rats is enhanced but manifested mostly as a spontaneous chaotic oscillation.<sup>6</sup> Since this spontaneous chaotic oscillation does not depend on the specific pressure wave form applied as forcing input, the obtained kernels and PDMs do not reflect this chaotic behavior. Thus, the contribution of the second PDM to the flow response in hypertensive rats should be interpreted only with respect to its causal relation with the applied pressure forcing stimulus, which does not include spontaneous oscillations. For

the same reason, the higher resting sympathetic tone in hypertensive rats will not be directly reflected on the kernels and PDM measurements.

## ACKNOWLEDGMENTS

This work was supported by NIH Grants No. RR-01861 (Biomedical Simulations Resource of the University of Southern California), No. HL-45623, and No. DR-15968, and by a grant from the Whitaker Foundation.

## APPENDIX

The kernel values obtained up to a maximum lag  $M$  (kernel memory) are combined to form a real symmetric  $(M+2) \times (M+2)$  square matrix:

$$Q = \begin{bmatrix} k_0 & \frac{1}{2}k_1(0) & \frac{1}{2}k_1(1) & \cdots & \frac{1}{2}k_1(M) \\ \frac{1}{2}k_1(0) & k_2(0,0) & k_2(0,1) & \cdots & k_2(0,M) \\ \frac{1}{2}k_1(1) & k_2(1,0) & k_2(1,1) & \cdots & k_2(1,M) \\ \vdots & \vdots & \vdots & \ddots & \vdots \\ \frac{1}{2}k_1(M) & k_2(M,0) & k_2(M,1) & \cdots & k_2(M,M) \end{bmatrix}, \quad (\text{A1})$$

that can be used to express the second-order Volterra model response,  $y_2(n)$  in a quadratic form:

$$y_2(n) = \underline{x}^T(n) Q \underline{x}(n), \quad (\text{A2})$$

where  $T$  denotes ‘‘transpose’’ and the  $(M+2)$ -dimensional vector  $\underline{x}^T(n) = [1x(n)x(n-1)\cdots x(n-M)]$  is composed of the stimulus  $(M+1)$ -point epoch at each time  $n$  and a constant 1 that allows incorporation of the lower order kernel contributions in Eq. (A2). Because  $Q$  is a real symmetric square matrix, there exists always an orthonormal matrix  $R$  such that  $Q = R^T \Lambda R$ , leading to the expression

$$y_2(n) = \underline{u}^T(n) \Lambda \underline{u}(n), \quad (\text{A3})$$

where  $\Lambda$  is the diagonal eigenvalue matrix and

$$\underline{u}(n) = R \underline{x}(n) \quad (\text{A4})$$

is the vector of transformed inputs by the orthonormal eigenvector matrix  $R$ . Inspection of the real eigenvalues in  $\Lambda$  allows selection of the significant ones on the basis of relative magnitude (a selection that calls for appropriate threshold criteria) and subsequent selection of the corresponding orthonormal eigenvectors that become the PDMs of this system.

For each significant eigenvalue  $\lambda_i$ , the values of the corresponding eigenvector  $\underline{\mu}_i^T = [\mu_{i,0} \mu_{i,1} \cdots \mu_{i,M+1}]$  (with the exception of  $\mu_{i,0}$ ) define the  $i$ th PDM:

$$p_i(m) = \sum_{j=1}^{M+1} \mu_{i,j} \delta(m-j+1), \quad (\text{A5})$$

where  $\delta(\bullet)$  denotes the discrete impulse function (Kronecker delta). The obtained  $i$ th PDM generates the  $i$ th mode output  $u_i(n)$  via convolution with the stimulus  $x(n)$ . Note that a constant offset value  $\beta_i = \mu_{i,0}$  must be added to the  $i$ th mode output  $u_i$  to express the second-order model prediction  $\hat{y}_2$  using  $J$  PDMs:

$$\hat{y}_2(n) = \sum_{i=1}^J \lambda_i [u_i(n) + \beta_i]^2. \quad (\text{A6})$$

Nonzero offset values  $\{\beta_i\}$  give rise to linear terms in terms of  $\{u_i\}$  in the model output equation. Note that the matrix  $Q$  is not positive definite and, therefore, negative and positive eigenvalues are possible.

In practice, the selection of the significant eigenvalues/eigenvectors must take into account signal-to-noise ratio (SNR) considerations (i.e., setting the selection threshold higher for lower SNR) and trade-offs between prediction accuracy and model complexity. A simple selection criterion is used in this study whereby the selected eigenvalues cumulatively account for at least 90% of the output signal power.

Clearly, when the actual system is of higher than second order, the search for PDMs based on the quadratic form of Eq. (A2) may be unduly confined. Nonetheless, the final model (which includes the estimated multi-input static nonlinearity) is not limited to the second order of the quadratic form employed, because the multivariate nonlinear function of the model (receiving as inputs the outputs of the  $J$  selected PDM filters) can be estimated up to any degree of nonlinearity. There is no guarantee that the PDMs selected from the quadratic model will be adequate for the high-order model; their adequacy will be assessed ultimately by the predictive ability of the resulting model.

Analytical evaluation of the static nonlinearity requires the introduction of a postulated mathematical structure containing certain unknown parameters that are subsequently estimated from the data via least-squares fitting. For instance, a multinomial structure of specified degree can be imposed [consistent with the modified Volterra expansion of Eq. (2)], and its coefficients can be estimated from the data through linear regression (because the unknown parameters enter linearly in this expression).

## REFERENCES

- <sup>1</sup> Amoroch, J., and A. Brandstetter. Determination of nonlinear functional response functions in rainfall runoff processes. *Water Resour. Res.* 7:1087–1101, 1971.
- <sup>2</sup> Billings, S. A., and G. N. Jones. Orthogonal least-squares parameter estimation algorithms for non-linear stochastic systems. *Int. J. Syst. Sci.* 23(7):1019–1032, 1992.
- <sup>3</sup> Chon, K. H., Y. M. Chen, N. H. Holstein-Rathlou, D. J. Marsh, and V. Z. Marmarelis. On the efficacy of linear system analysis of renal autoregulation in rats. *IEEE Trans. Biomed. Eng.* 40:8–20, 1993.
- <sup>4</sup> Chon, K. H., Y. M. Chen, V. Z. Marmarelis, D. J. Marsh, and N. H. Holstein-Rathlou. Detection of interactions between myogenic and TGF mechanisms using nonlinear analysis. *Am. J. Physiol.* 265:F160–F173, 1994.
- <sup>5</sup> Daniels, F. H., W. J. Arendshorst, and R. G. Roberds. Tubuloglomerular feedback and autoregulation in spontaneously hypertensive rats. *Am. J. Physiol.* 258:F1479–1489, 1990.
- <sup>6</sup> Holstein-Rathlou, N. H., and D. J. Marsh. A dynamical

- model of the tubuloglomerular feedback mechanism. *Am. J. Physiol.* 258:F1448–F1459, 1990.
- <sup>7</sup>Holstein-Rathlou, N. H., A. J. Wagner, and D. J. Marsh. Tubuloglomerular feedback dynamics and renal blood flow autoregulation in rats. *Am. J. Physiol.* 260:F53–F68, 1991.
- <sup>8</sup>Marmarelis, P. Z., and V. Z. Marmarelis. *Analysis of Physiological Systems: The White Noise Approach*. New York: Plenum, 1978.
- <sup>9</sup>Marmarelis, V. Z. A family of quasi-white random signals and its optimal use in biological system identification: Theory. *Biol. Cybern.* 27:49–56, 1977.
- <sup>10</sup>Marmarelis, V. Z. (Ed.) *Advanced Methods of Physiological System Modeling*. Los Angeles: USC, Biomedical Simulations Resource, 1987, Vol. I.
- <sup>11</sup>Marmarelis, V. Z. (Ed.) *Advanced Methods of Physiological System Modeling*. New York: Plenum, 1989, Vol. II.
- <sup>12</sup>Marmarelis, V. Z. Wiener analysis of nonlinear feedback in sensory systems. *Ann. Biomed. Eng.* 19:345–383, 1991.
- <sup>13</sup>Marmarelis, V. Z. Identification of nonlinear biological systems using Laguerre expansions of kernels. *Ann. Biomed. Eng.* 21:573–589, 1993.
- <sup>14</sup>Marmarelis, V. Z. (Ed.) *Advanced Methods of Physiological System Modeling*. New York: Plenum, 1994, Vol. III.
- <sup>15</sup>Marmarelis, V. Z. Modeling methodology for nonlinear physiological systems. *Ann. Biomed. Eng.* 25:239–251, 1997.
- <sup>16</sup>Marmarelis, V. Z., K. H. Chon, Y. M. Chen, N. H. Holstein-Rathlou, and D. J. Marsh. Nonlinear analysis of renal autoregulation under broadband forcing conditions. *Ann. Biomed. Eng.* 21:591–603, 1993.
- <sup>17</sup>Marsh, D. J., J. L. Osborne, and A. W. Cowley.  $1/f$  Fluctuations in arterial pressure and regulation of renal blood flow in dogs. *Am. J. Physiol.* 258:F1394–F1400, 1990.
- <sup>18</sup>Sakai, T., E. Hallman, and D. J. Marsh. Frequency domain analysis of renal autoregulation in the rat. *Am. J. Physiol.* 250:F364–F378, 1986.
- <sup>19</sup>Volterra, V. *Theory of Functions and of Integral and Integro-Differential Equations*. New York: Dover, 1930.
- <sup>20</sup>Watanabe, W., and L. Stark. Kernel method for nonlinear analysis: Identification of a biological control system. *Math. Biosci.* 27:99–109, 1975.
- <sup>21</sup>Wiener, N. *Nonlinear Problems in Random Theory*. New York: The Technology Press of MIT and Wiley, 1958.
- <sup>22</sup>Zhu, Q. M., and S. A. Billings. Fast orthogonal identification of nonlinear stochastic models and radial basis function neural networks. *Int. J. Control* 64(5):871–886, 1996.